2015 European Conference on Circuit Theory and Design (ECCTD)

Analysis to Optimize Sensitivity of RF Energy Harvester with Voltage Boost Circuit

Dan Luo, Hiroshi Fuketa, Kenichi Matsunaga*, Hiroki Morimura*, Makoto Takamiya, and Takayasu Sakurai
Institute of Industrial Science, The University of Tokyo, 4-6-1 Komaba, Meguro-ku, Tokyo, Japan, 153-8505
*) NTT Device Technology Laboratories, NTT Corporation
e-mail: {luodan, tsakurai}@iis.u-tokyo.ac.jp

***Abstract*— Analytical theory and simulation-based analysis for optimizing sensitivity of RF energy harvester are discussed. A target harvester is a widely-used MOSFET Dickson charge-pump harvester from a small-signal RF power with a voltage booster at the front end. Charging time is also analyzed. Derived expressions show good match with simulation results. The results provide an insight for design optimization based on circuit and device parameters.**

Keywords—Energy harvester, Voltage booster, Modeling, Subthreshold slope, Optimization

LIST OF SYMBOLS

C_1	Equivalent capacitance of one charge-pump MOS
C_N	Equivalent capacitance of total charge pump
C_C	Coupling capacitance in charge-pump circuit
f	Frequency of input RF signal
I_0	Current coefficient of charge-pump MOS
I_{DS}	Drain current of a charge-pump MOS
L	Inductance of an inductor in booster
m	Subthreshold drain voltage coefficient
n	Subthreshold gate voltage coefficient
N	Number of MOS stages of charge pump
Q_1	Charge transferred in one cycle by one charge-pump stage
R	Equivalent resistance of antenna
R_1	Equivalent resistance of charge-pump MOS
R_N	Equivalent resistance of total charge pump
T	Cycle time
U_T	Thermal voltage
V_{DS}	Drain-Source voltage of charge-pump MOS
V_{GS}	Gate-Source voltage of charge-pump MOS
V_{IN}	Amplitude of input signal to charge pump
V_O	DC voltage of single charge-pump stage
V_{OUT}	Output DC voltage after charge pump
V_{RF}	Amplitude of input RF signal
V_{TH}	Threshold voltage of charge-pump MOS
ω	Angular frequency of input RF signal
Z_1	Effective impedance of one charge-pump stage

I. INTRODUCTION

Recently, energy harvesting from small RF signal is drawing attention as a possible energy source for Internet of Things (IoT) nodes [1]. Input RF signal is as small as -30dBm, which corresponds to 7mV if antenna resistance is 50Ω. Modeling and optimization of the harvester are discussed in this paper. The harvesters under consideration are based on Dickson charge pump circuit with a voltage booster of, either LC-type or CL-type, in the front-end, which are depicted in Fig.1.

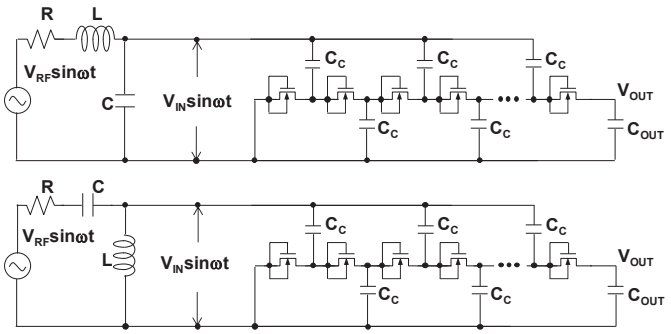

Fig. 1. Dickson charge pump with an LC booster (top) and a CL booster (bottom) considered in this paper. Phases of sinusoidal waves are omitted as they are not relevant in this paper.

II. MODELING

A. Modeling of MOSFET

Since the input RF voltage is small, the MOSFET in a charge pump circuit is operated in a subthreshold region, and thus the *I-V* characteristics of a MOSFET with a forward-biased junction used in the charge pump is modeled as follows.

$$I_{DS} = I_0 e^{\frac{V_{GS}-V_{TH}}{nU_T}} \left(1 - e^{-\frac{V_{DS}}{mU_T}}\right) \quad (1)$$

Introduction of m is necessary to fit the SPICE MOS model calculation. As an added benefit, m makes it possible to model steep-S devices including a Tunneling FET based circuits in the future [2, 3]. Two types of transistors are used in this paper namely Zero-V_{TH} and Low-V_{TH}, to show the generality of the analysis. *I-V* characteristics are shown in Fig. 2.

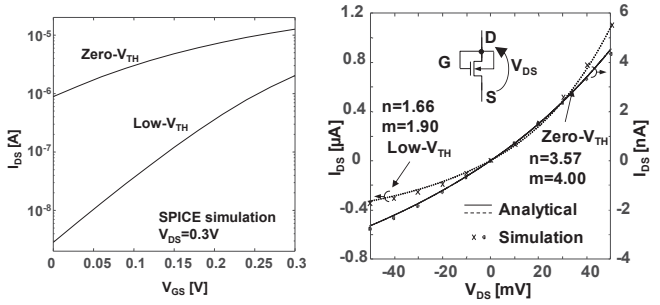

Fig. 2. Employed MOSFETs are two types for 0.25μm CMOS, namely zero-V_{TH} and low-V_{TH}. (a) Subthreshold *I-V* characteristics by SPICE model and (b) analytical model (1) fitted to SPICE model of diode-connected MOSFET. Fitted parameters are shown in the figure. Both of the gate width and length are the allowed minimum. All SPICE simulations in this paper use the same gate length and width as they are supposed to be appropriate for achieving the best sensitivity.

B. Modeling of One Charge-Pump Stage

A Dickson charge pump circuit in Fig. 1 consists of multiple of diode-connected MOS transistor stages whose single stage is depicted in Fig. 3(a). Since C_C is chosen to be very large, it is transparent to RF signal and then the input waveform to a MOS diode is schematically shown in Fig. 3(b). Obtaining an expression for the DC voltage, V_O, and an equivalent impedance for one charge-pump stage are the aims of this section.

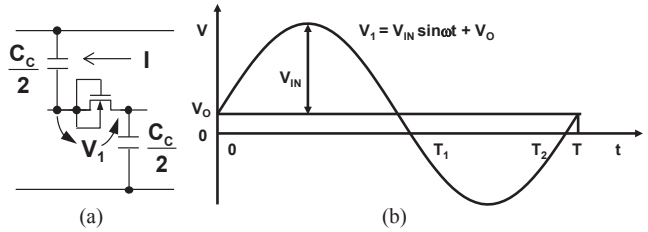

(a) (b)

Fig. 3. (a) One charge-pump stage and (b) input waveform to diode-connected MOSFET. T_1 and T_2 denotes the time when V=0.

When input swing is very small, V_O is small and thus $T_1 \approx T/2$ and $T_2 \approx T$ hold. In this case, the charge transferred from right to left in one cycle, Q_1, is calculated as follows. Q_1 should be zero at the steady state.

$$Q_1 = \int_0^{T/2} I_0 e^{-\frac{V_{TH}}{nU_T}} (1 - e^{-\frac{V_1}{mU_T}}) dt - \int_{T/2}^{T} I_0 e^{\frac{-V_1 - V_{TH}}{nU_T}} (1 - e^{-\frac{-V_1}{mU_T}}) dt \quad (2)$$

$$V_1 = V_{IN} \sin \omega t + V_O \quad (3)$$

Putting $x = (V_{IN} / U_T) \sin \omega t$ and $y = V_O / U_T$, and considering only the sign of the sinusoidal wave changes between the former half and the latter half of a cycle, the following holds.

$$Q_1 = I_0 e^{-\frac{V_{TH}}{nU_T}} \int_0^{T/2} \left[(1 - e^{\frac{-y-x}{m}}) - e^{\frac{-y+x}{n}} (1 - e^{\frac{y-x}{m}}) \right] dt \quad (4)$$

When the function in the integral is expanded in terms of x and y around zero assuming both x and y are small, the following expression holds.

$$Q_1 \approx I_0 e^{-\frac{V_{TH}}{nU_T}} \int_0^{T/2} \left(-\frac{x^2}{mn} + \frac{2y}{m} \right) dt = \frac{TI_0}{m} e^{-\frac{V_{TH}}{nU_T}} \left(-\frac{V_{IN}^2}{4nU_T^2} + \frac{V_O}{U_T} \right) \quad (5)$$

By setting Q_1=0, output DC voltage V_O is solved as follows.

$$\frac{V_O}{U_T} = \frac{1}{4n} \left(\frac{V_{IN}}{U_T} \right)^2 \quad (6)$$

The above expression is simple yet excellent in reproducing the simulation results as is seen in Fig. 4. This expression for the first time explains the importance of steepness, n, in the subthreshold region and steep-S devices for a harvester.

When V_{IN} gets very large, the above approximation is not valid any more. In that case, though, it can be understood from a physical consideration that V_O asymptotes to V_{IN}, that is, $V_O \sim V_{IN}$. Connecting this linear dependence of V_O on V_{IN} and the quadratic dependence (6) smoothly, the expression which is valid for all range of V_{IN} is derived as follow whose effectiveness is shown in Fig.4.

$$\frac{V_O}{U_T} = \frac{V_{IN}}{U_T} \left(1 - e^{-\frac{V_{IN}}{4nU_T}} \right) \quad (7)$$

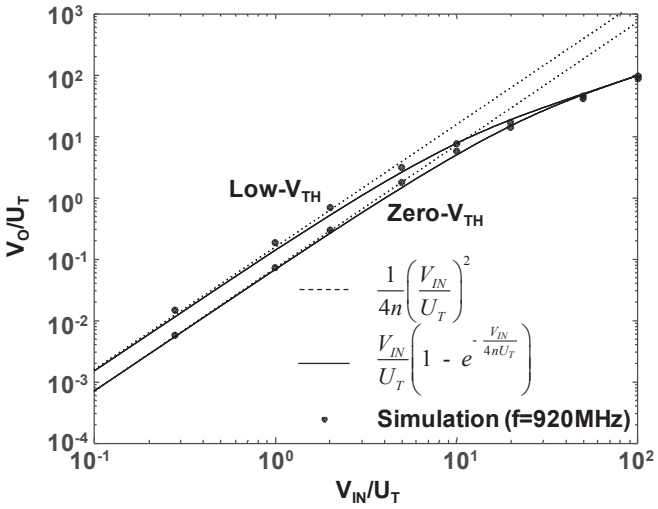

Fig. 4. Comprison of theoretical calculation using (6) and (7) and simulation results for output DC voltage of single charge-pump stage.

One more thing that is necessary to model the single pumping stage is to obtain an equivalent impedance, Z_1, which is seen from a booster circuit. It turns out that Z_1 can be expressed as a parallel connection of resistance, R_1, and capacitance, C_1 as is shown in Fig.5. This situation is verified from Fig. 6, where the real part of $1/Z_1$ is shown to be constant and the imaginary part is proportional to f. R_1 is expressed as below using the device parameters in (1).

$$\frac{1}{R_1} = \left. \frac{dI_{DS}(V_{GS} = V_{DS} = V)}{dV} \right|_{V=0} = \frac{I_0}{mU_T} e^{-\frac{V_{TH}}{nU_T}} \quad (8)$$

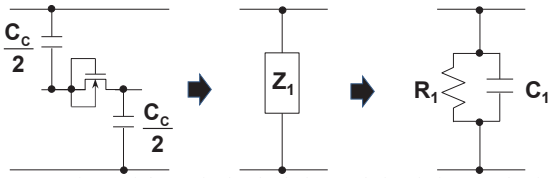

Fig. 5. Comprison of theoretical calculation and simulation results for output DC voltage of single charge-pump stage.

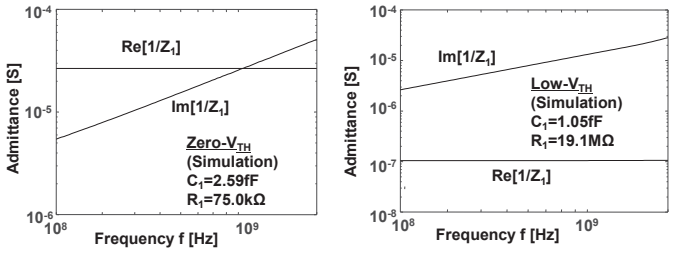

(a) (b)

Fig. 6. Frequency dependence of real and imaginary part of $1/Z_1$ for (a) Zero-V_{TH} MOSFET and (b) Low-V_{TH} MOSFET.

C. Modeling of Charge pump with Voltage Booster

Now, a total harvester is modeled. Two types of a voltage booster are considered here, namely LC type and CL type, whose equivalent circuit is shown in Fig. 7. R_N and C_N respectively represent total equivalent resistance and capacitance of a charge-pump circuit consisting of N stages, or in other words, N diode-connected MOSFET's. R_N and C_N can be expressed as follows. Note that R_N is not $N \times R_1$ but R_1/N.

$$R_N = R_1 / N,\ C_N = N C_1 \tag{9}$$

Output capacitance, C_{OUT}, in Fig. 1 comes in series to R_N and C_N and thus can be neglected as in Fig. 7, when C_{OUT} is large, which is the case in consideration here.

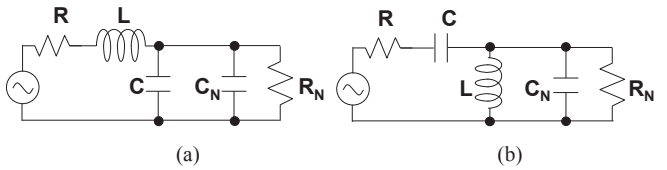

(a) (b)

Fig. 7. Equivalent circuit of total harvester with (a) LC-type booster and (b) CL-type booster

Transfer function of boosters, H, from V_{RF} to V_{IN} in Fig. 1 can be written as follows.

$$H_{LC} = \frac{1}{L(C+C_N)s^2 + \left(\frac{L}{R_N} + R\left(C+C_N\right)\right)s + \frac{R}{R_N} + 1} \tag{10}$$

$$H_{CL} = \frac{LCs^2}{RLCC_N s^3 + \left(\frac{R}{R_N}LC + L\left(C+C_N\right)\right)s^2 + \left(\frac{L}{R_N} + RC\right)s + 1} \tag{11}$$

The subscript LC and CL correspond to the booster type. Square of the absolute value of the transfer function, $|H|^2$, has the following form with s', ω', Q, a, being normalized Laplace variable, normalized angular frequency, Q value, and a real number, respectively.

$$\left|H_{LC}\right|^2 \propto \left|\frac{1}{s'^2 + s'/Q + 1}\right|^2_{s'=j\omega'} = \frac{1}{(1-\omega'^2)^2 + \omega'^2/Q^2} \tag{12}$$

$$\left|H_{CL}\right|^2 \propto \left|\frac{s'^2}{as'^3 + s'^2 + s'/Q + 1}\right|^2_{s'=j\omega'} = \frac{\omega'^4}{(1-\omega'^2)^2 + (1/Q - a\omega'^2)^2\omega'^2} \tag{13}$$

Seeing (6), $|H|^2$ should be maximized to get the best boosting effect but unfortunately the exact condition to maximize $|H|^2$ is difficult to express analytically. It is found, however, a condition that the real part of the denominator of H is zero can be a good approximation for maximizing $|H|^2$, whose situation is shown in Figs. 8 and 9.

This condition corresponds to $\omega' = 1$ in (12) and (13). The relative error of the approximated $|H|^2$ value is within 3% compared with the exact maximum when Q value is more than 3. This range of Q value is usually adopted since the voltage boosting effect is expected anyway when a booster is deployed.

Considering R_1 values in Fig. 6 and $R \approx 50\Omega$ and using (9), it is seen that $R / R_N \ll 1$ holds. In this situation, $|H|^2$ maximizing condition becomes the following for both LC and CL types.

$$L(C + NC_1)\omega^2 = 1 \tag{14}$$

This can be achieved by tuning L and C with circuit techniques. Input AC voltage to a charge pump block, V_{IN}, is calculated as

$$V_{IN}{}^2 = \left|H\right|^2 V_{RF}{}^2 . \tag{15}$$

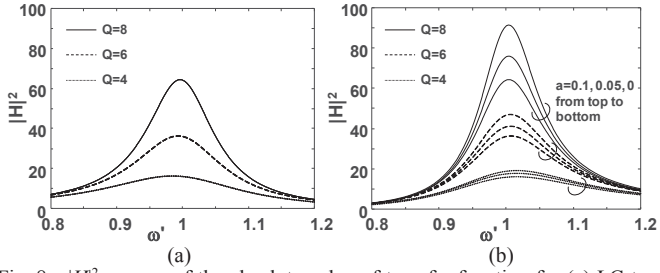

(a) (b)

Fig. 8. $|H|^2$, square of the absolute value of transfer function for (a) LC-type booster using (12) and (b) CL-type booster using (13).

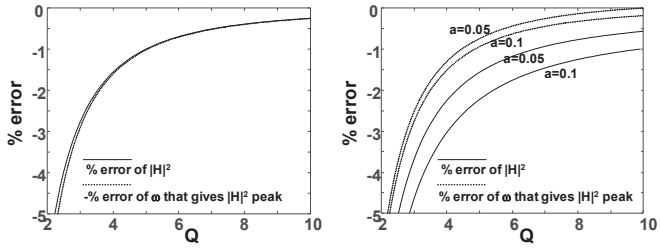

(a) (b)

Fig. 9. Relative error of approximated maximum and true maximum of $|H|^2$ for (a) LC-type booster using (12) and (b) CL-type booster using (13).

Output DC voltage, V_{OUT}, of the total charge pump consisting of N stages is expressed as a simple sum of each single-stage DC voltage.

$$V_{OUT} = NV_O \tag{16}$$

Using above formulas and (6) yield the following expression for V_{IN} and V_{OUT}.

$$V_{IN,LC} = \frac{1}{\left(N\frac{L}{R_1} + \frac{R}{L\omega^2}\right)\omega} V_{RF} \tag{17}$$

$$V_{IN,CL} = \frac{L\left(1 - NLC_1\omega^2\right)\omega}{NL^2\omega^2 / R_1 + R\left(1 - NLC_1\omega^2\right)^2} V_{RF} \tag{18}$$

$$\frac{V_{OUT,LC}}{U_T} = \frac{N}{4n}\left(\frac{V_{IN}}{U_T}\right)^2 = \frac{N}{4n}\frac{1}{\left(N\frac{L}{R_1} + \frac{R}{L\omega^2}\right)^2\omega^2}\left(\frac{V_{RF}}{U_T}\right)^2 \tag{19}$$

$$\frac{V_{OUT,CL}}{U_T} = \frac{N}{4n}\left(\frac{L\left(1 - NLC_1\omega^2\right)\omega}{NL^2\omega^2 / R_1 + R\left(1 - NLC_1\omega^2\right)^2}\right)^2\left(\frac{V_{RF}}{U_T}\right)^2 \tag{20}$$

V_{OUT} is a function of number of charge-pump stages, N. Differentiating by N and putting the derivative to zero, the optimum stage count, N_{OPT}, can be obtained as follows.

$$N_{OPT,LC} = \frac{RR_1}{L^2\omega^2} \tag{21}$$

$$N_{OPT,CL} = \frac{L/R_1 + 2RC_1 - \sqrt{\left(L/R_1\right)\left(L/R_1 + 4RC_1\right)}}{2RLC_1{}^2\omega^2} \tag{22}$$

There is an optimum value for N because if N increases, R_N gets small and this in turn decreases the voltage boosting efficiency although the charge pump multiplies V_{IN} more.

When N_{OPT} is employed, output voltage of the harvester is maximized and reaches following $V_{OUT,OPT}$ for both of LC and CL. This corresponds to the sensitivity of a harvester for small

RF signal with $R_1/4R$ being a voltage boosting effect understood from (6).

$$\frac{V_{OUT,OPT}}{U_T} = \frac{1}{16n}\frac{R_1}{R}\left(\frac{V_{RF}}{U_T}\right)^2 \quad (23)$$

When V_{RF} is considerably large, (7) instead of (6) should be used and the numerical calculation is needed rather than pure analytical treatment but for most of the cases, (6) is sufficiently good because the RF signal is usually less than $5U_T$.

D. Modeling of Charging Time.

Charging waveform, $V_{OUT}(t)$, of the output capacitance, C_{OUT}, can be derived by using (2) and (5) while noting that V_O obtained in (6) is a final steady state value but in general V_O changes in time. Assuming C_{OUT} very large, the following holds.

$$C_{OUT}\frac{dV_{OUT}(t)}{dt} = -\frac{Q_1(V_O = V_{OUT}/N)}{T} = -\frac{1}{NR_1}\left(V_{OUT}(t) - V_{OUT}\right) \quad (24)$$

$$V_{OUT}(t) = V_{OUT}\left(1 - e^{-\frac{t}{NR_1C_{OUT}}}\right) = V_{OUT}\left(1 - e^{-\frac{t}{\tau}}\right) \quad (25)$$

The charging time constant τ is NR_1C_{OUT}, which turns out to be independent from f.

III. Comparison with SPICE Simulation and Conclusion

Analytical expressions for V_{IN}, a boosted AC voltage which is an input to a charge pump, and V_{OUT}, a DC output voltage of an energy harvester, are obtained as (17) through (20). These analytical calculations are compared with SPICE simulation results in Figs. 10-13 for two boost types and MOS types. f=920MHz and L=100nH. Overall agreement is satisfactory for boosting efficiency, V_{IN}/V_{RF}, and sensitivity of a harvester, V_{OUT}/V_{RF}. Hence, the optimum number of stages, N_{OPT}, is also in accordance with SPICE simulation. Charging time (25) also fits very well with simulation as shown in Fig. 14.

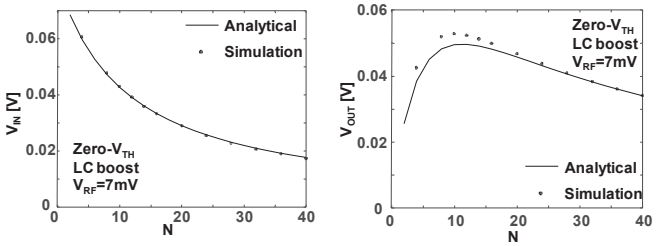

Fig. 10. Comparison of analytical expressions, (17) and (19), and SPICE simulation results. for (a) V_{IN} and (b) V_{OUT} for LC-type voltage boost with Zero-V_{TH} MOS.

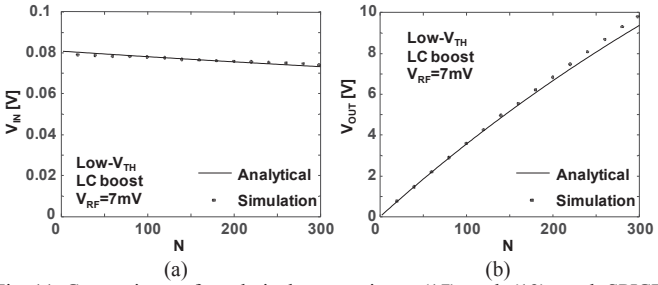

Fig. 11. Comparison of analytical expressions, (17) and (19), and SPICE simulation results. for (a) V_{IN} and (b) V_{OUT} for LC-type voltage boost with Low-V_{TH} MOS. For this configuration, N can not be very large as C becomes minus in (14).

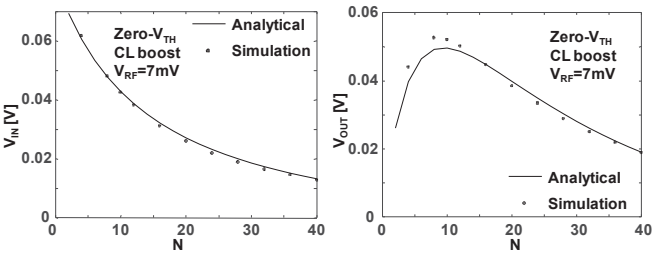

Fig. 12. Comparison of analytical expressions, (18) and (20), and SPICE simulation results. for (a) V_{IN} and (b) V_{OUT} for CL-type voltage boost with Zero-V_{TH} MOS.

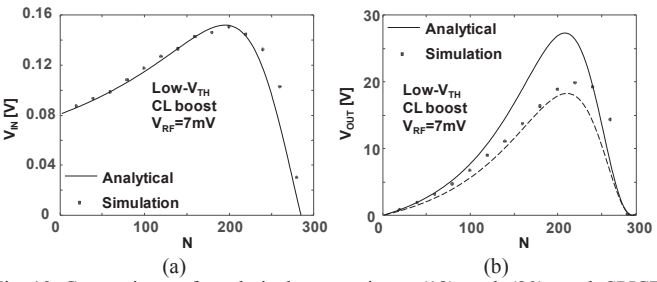

Fig. 13. Comparison of analytical expressions, (18) and (20), and SPICE simulation results. for (a) V_{IN} and (b) V_{OUT} for CL-type voltage boost with Low-V_{TH} MOS. Broken line in (b) is analytical calculation using more complex but more accurate expression (7).

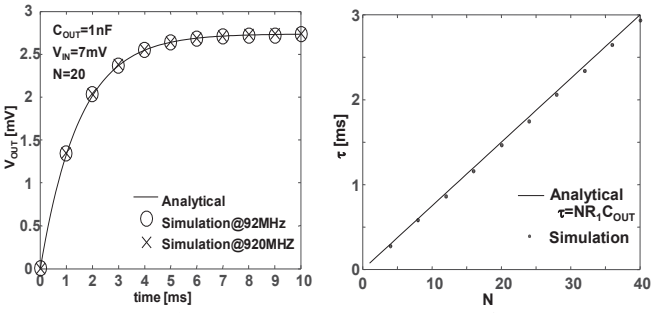

Fig. 14. (a) Simulated waveform of charging C_{OUT} and (b) comparison of analytical expression and SPICE simulation results.

Several simple yet useful analytical expressions such as (6), (23), and (25) are obtained for a widely-used charge-pump based RF energy harvester. As they reproduce well the SPICE simulation results, they can be used in optimizing a harvester at the early stage of the design.

References

[1] S. Oh and D. D. Wentzloff, "A -32dBm Sensitivity RF Power Harvester in 130nm CMOS," IEEE Radio Frequency Integrated Circuits Symposium, pp.483-486, 2012.

[2] H. Fuketa, K. Yoshioka, K. Fukuda, T. Mori, H. Ota, M. Takamiya, and T.Sakurai, "Design Guidelines of Steep Subthreshold TFET to Minimize Energy of Logic Circuits," International Conference on Solid State Devices and Materials (SSDM), pp. 832-833, Sep. 2014.

[3] H. Fuketa, K. Yoshioka, K. Fukuda, T. Mori, H. Ota, M. Takamiya, and T. Sakurai, "Design Guidelines to Achieve Minimum Energy Operation for Ultra Low Voltage Tunneling FET Logic Circuits," Japanese Journal of Applied Physics, vol. 54, no. 4S, 04DC04, Apr. 2015.